Photochemically Induced Isothermal Phase Transition in Polymer Liquid Crystals with Mesogenic Phenyl Benzoate Side Chains. 1. Calorimetric Studies and Order Parameters

Tomiki Ikeda,* Shin Horiuchi, Durga B. Karanjit, Seiji Kurihara, and Shigeo Tazuke†

Photochemical Process Division, Research Laboratory of Resources Utilization, Tokyo Institute of Technology, 4259 Nagatsuta, Midori-ku, Yokohama 227, Japan.
Received October 3, 1988; Revised Manuscript Received April 20, 1989

ABSTRACT: In order to explore photochemically induced isothermal phase transition behaviors of polymer liquid crystals (PLC) with mesogenic phenyl benzoate side chains in relation to their morphological properties, orientational ordering of the PLC's was studied by means of calorimetric measurements and order parameter (S) determinations by FT-IR dichroism. The PLC samples studied are poly(4'-methoxyphenyl 4-((acryloyloxy)alkoxy)benzoate) (PAPBn) in which the alkyl spacer length $(CH_2)_n$ was varied as n = 2, 3, 5, or 6 and their copolymers with 4'-methoxy-4-((acryloyloxy)alkoxy)azobenzene (AAZOm) where m = 2, 3, 5, 6, or 11 (poly(APBn-*co*-AAZOm) or copolymer n-m). Calorimetric studies revealed that PAPB3 exhibited particularly low values of T_{NI} (nematic to isotropic phase transition temperature), ΔH_{NI} (enthalpy change at N-I transition), and ΔS_{NI} (entropy change at N-I transition). Furthermore, these quantities were strongly dependent on molecular weight (MW) and spacer length (n). In copolymer n-m, copolymer 3-3 possessed the lowest values of ΔH_{NI} and ΔS_{NI}, which were even lower than those of PAPB3. IR dichroic studies have shown a parallel relationship between ΔS_{NI} and S. Namely, among the homopolymers, PAPB3 showed the smallest S and among the copolymers copolymer 3-3 possessed the smallest S. The S value of copolymer 3-3 was further lower than that of PAPB3, indicating that copolymer 3-3 has the least orientational ordering in the N state among the PLC samples examined.

Introduction

Vision is the most sensitive photoresponsive system occurring in nature.[1] Absorption of photons results in cis-trans isomerization of the photoreceptor (retinal) in rhodopsin. This structural perturbation occurring in the local site of rhodopsin induces conformational change of the whole protein molecules, resulting in subsequent amplification of the incident photosignals.[1] We applied this principle to photoimage storage devices and have demonstrated several examples of the photochemically induced phase transition.[2-6] They are in micellar,[2] vesicular,[2,3] and liquid-crystalline systems.[4-6]

Polymeric materials may be the best choice for supporting materials. Many photochromic compounds are doped in the polymeric materials for efficient performance of the photoresponsive systems,[7-9] and in fact, polymer binders are essential for the practical use of the systems. Another advantage of polymeric materials is a phenomenon of glass transition of polymers. Below the glass transition temperature (T_g), the segmental motion of the polymer chains is frozen-in, and thus the stored information can expectedly be kept stable for a long period. We proposed this image fixation process by freezing molecular motion in polymer matrices over 10 years ago.[10]

Use of polymer liquid crystals (PLC) for image storage materials has been reported by several groups.[11-16] Shibaev et al.[11] and Coles and Simon[12] reported the laser-addressed PLC storage displays in which heat-mode writing was exclusively employed. Furthermore, dye chromophores were incorporated into the PLC's to enhance "heat" absorption.[12] Photon-mode image storage in the PLC was first demonstrated by Eich and Wendorff as "holographic" optical storage.[15,16] In their system, photoirradiation caused isomerization of the photochromic groups (azobenzene derivatives) incorporated into the PLC's, inducing simultaneously "grating" in the PLC. The "grating" was constructed essentially by the change in the refractive index resulting from the photoisomerization.[15,16]

In this paper, we report calorimetric studies and order parameter determination of the host PLC's used in our study for the image storage materials. The aim of this work is to provide information on the orientational ordering of the liquid-crystalline state of the PLC's, which was expected to be closely relatd to the photochemically induced phase transition behaviors. Our system is different from the previous works in that *photochemically induced isothermal phase transition of the matrix PLC's* is the principle involved in the image storage system. This study is essential to construct highly efficient image storage systems based on PLC's.

Experimental Section

Materials. Structure of the PLC's used in this study is shown in Figure 1. Acrylates with mesogenic phenyl benzoates in the side chain (APBn) were prepared by the method reported by Ringsdorf et al.,[17] and the acrylates with side-chain azobenzene moieties (AAZOm) were synthesized by a similar method to that employed by Ringsdorf et al.[18] Analytical results are shown below.

APB2: mp 93.1-93.5 °C; IR (KBr) 2950, 1710, 1600, 1500 cm^{-1}; ^1H NMR ($CDCl_3$) δ 3.80 (s, 3 H), 4.30 (m, 2 H), 4.50 (m, 2 H), 5.85 (m, H), 6.25 (m, 2 H), 7.00 (m, 6 H), 8.10 (d, 2 H).

APB3: mp 74.0-74.5 °C; IR (KBr) 2950, 1710, 1600, 1500 cm^{-1}; ^1H NMR ($CDCl_3$) δ 2.15 (m, 2 H), 3.84 (s, 3 H), 4.32 (m, 4 H), 5.95 (m, H), 6.25 (m, 2 H), 7.14 (m, 6 H).

APB5: mp 62.2-62.5 °C; IR (KBr) 2950, 1720, 1600, 1500 cm^{-1}; ^1H NMR ($CDCl_3$) δ 1.7-2.1 (m, 6 H), 3.75 (s, 3 H), 4.16 (m, 4 H), 5.85 (m, H), 6.15 (m, 2 H), 7.00 (m, 6 H), 8.16 (d, 2 H).

APB6: mp 53.0-53.5 °C; IR (KBr) 3000, 1720, 1600, 1500 cm^{-1}; ^1H NMR ($CDCl_3$) δ 1.2-2.1 (m, 8 H), 3.70 (s, 3 H), 4.16 (m, 4 H), 5.85 (m, H), 6.15 (m, 2 H), 7.00 (m, 6 H), 8.16 (d, 2 H).

AAZO3: mp 91.2-92.3 °C; IR (KBr) 2930, 1730, 1595, 1580, 1490 cm^{-1}; ^1H NMR ($CDCl_3$) δ 2.0-2.5 (m, 2 H), 3.85 (s, 3 H), 4.13 (t, 2 H), 4.37 (t, 2 H), 5.7-6.6 (m, 3 H), 6.97 (d, 4 H), 7.83 (d, 4 H).

† Deceased July 11, 1989.

0024-9297/90/2223-0036$02.50/0

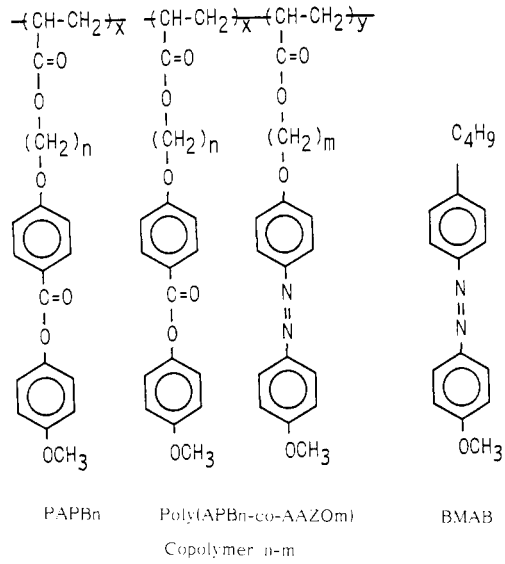

Figure 1. Structure of liquid crystals used in this study.

AAZO6: mp 94.8–95.5 °C; IR (KBr) 3410, 2930, 1710, 1595, 1580, 1495 cm^{-1}; ^1H NMR ($CDCl_3$) δ 1.5–2.0 (m, 8 H), 3.87 (s, 3 H), 4.0–4.4 (m, 4 H), 5.7–6.6 (m, 3 H), 7.05 (d, 4 H), 7.95 (d, 4 H).

AAZO11: mp 80.5–82.4 °C; IR (KBr) 3400, 2930, 1720, 1595, 1580, 1495 cm^{-1}; ^1H NMR ($CDCl_3$) δ 1.1–1.9 (m, 18 H), 4.0–4.3 (m, 4 H), 5.7–6.6 (m, 3 H), 6.98 (d, 4 H), 7.88 (d, 4 H).

4-Butyl-4′-methoxyazobenzene (BMAB) was prepared and purified as reported previously.[4]

Polymerization was conducted in tetrahydrofuran (THF) by the use of azobis(isobutyronitrile) (AIBN) as an initiator. Benzene was also used in place of THF when high molecular weight polymers were prepared. In copolymerization, conversion was always kept low (<15%). All polymers were purified by repeated precipitation from chloroform solution into cold ether.

Characterization of Polymers. Molecular weight (MW) of the polymers was determined by gel permeation chromatography (GPC; Toyo Soda HLC-802, column, GMH6 × 2 + G4000H8 + G2500H8; eluent, chloroform) calibrated with standard polystyrenes. GPC was also employed for fractionation of the polymers using preparative columns. Liquid crystalline behavior and phase transition behavior was examined on an Olympus Model BHSP polarizing microscope equipped with a Mettler hot-stage Model FP-80 or FP-82. Thermotropic properties of the polymers were determined with a differential scanning calorimeter (SEIKO I&E SSC-5000) at a heating rate of 10 °C/min. At least four scans were performed for each sample to check reproducibility.

Composition of the copolymers was determined by absorption spectroscopy based on molar extinction coefficients of the azo monomers separately determined.

Polarized IR spectra were recorded with a JEOL JIR-3505 FT-IR spectrometer with the aid of a gold wire glid polarizer. Oriented samples of the PLC films for the FT-IR measurements were prepared by casting the polymer solution in chloroform onto CaF_2 plates. Two methods were employed for orientation: rubbing treatment and orientation in magnetic field. In the rubbing treatment, the CaF_2 plates were coated with poly(vinyl alcohol), and after the resulting plates were dried completely, the surface of the plates were rubbed with a fine sandpaper along one direction. On the plates thus prepared, the PLC solution was cast and dried under vacuum. Surface of the PLC was covered with an additional CaF_2 plate for the measurements. The samples were subjected to annealing just below T_{NI} of the PLC. Homogeneous orientation was confirmed for these PLC films by polarizing microscopy.

Orientation of the PLC films in the magnetic field was performed by placing the cast film in the magnetic field of 2.1 T. The film was heated in the magnetic field above T_{NI} of the sample and cooled gradually just below the phase transition temperature, and the sample was kept at this temperature for 5 h. Homogeneous orientation was also confirmed for these samples. It is noteworthy that the PLC films oriented in the magnetic field showed much better orientation than those prepared by the rubbing treatment. This was confirmed by the polarizing microscopy. When the sample was rotated between a pair of the crossed polarizers, the intensity of the transmitted light changed depending on the angle between the directions of the polarizer and the orientation of the sample. The PLC films oriented in the magnetic field showed a marked contrast between parallel (or perpendicular) and a 45° direction compared with the samples obtained by the rubbing treatment, indicating better orientation of the former.

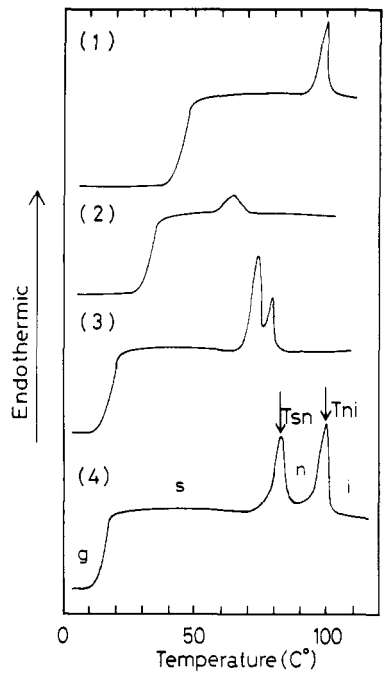

Figure 2. DSC thermograms observed for PAPB*n*: (1) PAPB2; (2) PAPB3; (3) PAPB5; (4) PAPB6. Abbreviations: g, glassy state; n, nematic; s, smectic; i, isotropic melt. Heating rate was 10 °C/min.

Results and Discussion

DSC Thermograms. In Figure 2 are shown typical DSC thermograms observed for the homopolymers PAPB*n* (n = 2, 3, 5, and 6) with M_n = ~4000, which were those on heating. In each measurement, the sample was heated to a temperature ~50 °C higher than T_{NI} of the sample, then gradually cooled down to a temperature just below T_{NI}, and kept for 1 h at this temperature for annealing. For PAPB2 and PAPB3, we observed two endothermic events: one occurring at lower temperature as a shift of the base line toward endothermic direction is due to glass transition of the polymers (T_g) and the other corresponds to nematic (N) to isotropic (I) phase transition of the polymer liquid crystals (T_{NI}). We confirmed the N phase with the polarizing microscope. The homopolymers with longer alkyl spacers, PAPB5 and PAPB6, exhibited an additional endothermic peak between T_g and T_{NI} which corresponds to smectic (S) to N phase transition. A characteristic feature seen in the DSC thermograms of the homopolymers is that PAPB3 shows a broader peak of T_{NI}; thus this PLC exhibits a somewhat wider range for the biphasic temperature than the other homopolymers.

Effect of Molecular Weight (MW). In order to examine the MW effect of the homopolymers on the thermotropic properties, nearly monodispersed polymer samples with varying MW's were subjected to DSC measurements. Here, the polydispersity index (M_w/M_n) of the samples was in the range of 1.0–1.3. Figure 3 shows the

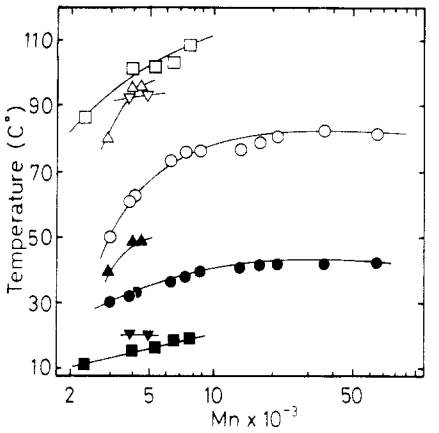

Figure 3. Phase transition behaviors of PAPB*n* as a function of molecular weight. PAPB2: (▲), T_g; (△), T_{NI}. PAPB3: (●), T_g; (○), T_{NI}. PAPB5: (▼), T_g; (▽), T_{NI}. PAPB6: (■), T_g; (□), T_{NI}.

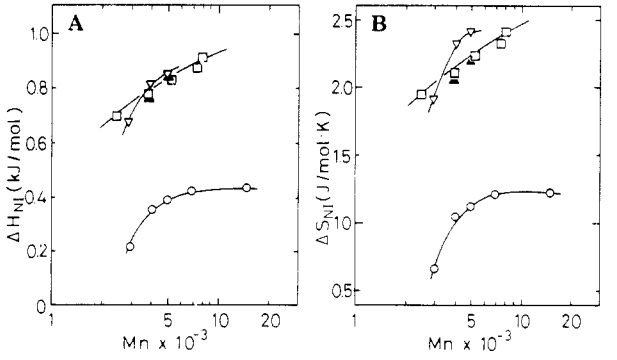

Figure 4. Thermodynamic data on N→I phase transition of PAPB*n* as a function of molecular weight: A, ΔH_{NI}; B, ΔS_{NI}; (▽), PAPB2; (○), PAPB3; (▲), PAPB5; (□), PAPB6.

phase transition behaviors of the PLC's as a function of MW. None of the monomers (APB*n*) exhibited a liquid-crystalline phase. With increasing MW, T_g and T_{NI} of the polymers increased in the low MW region up to $M_n \sim 10^4$ and reached constant values at MW > 10^4.

In Figure 4, thermodynamic data on the N→I phase transition of PAPBn (ΔH_{NI} and ΔS_{NI}) are shown as a function of MW. As in the case of T_g and T_{NI}, both ΔH_{NI} and ΔS_{NI} increased with MW in all polymers up to $M_n \sim 10^4$. These trends were already observed in poly(methylsiloxane) with side-chain phenyl benzoate mesogens[19] and in the main-chain PLC's.[20] One possible explanation for the MW effect is the effect of the initiators attached to the ends of the polymer chains. When MW is low, the relative contribution of the end groups is large compared with those of high MW. Thus, in the low MW polymers, order of the LC phase is reduced owing to the end groups.

Effect of Alkyl Spacer Length (*n*). In Figure 5, phase transition temperatures of PAPB*n* with $M_n = \sim 4000$ are ploted as a function of the number of the methylene units in the spacer chain (n). In Figure 6, similar plots on ΔH_{NI} and ΔS_{NI} are indicated. It is clearly seen that T_g of PAPB*n* decreased rather monotonically with increasing the spacer length n, while T_{NI} exhibited an odd–even effect with n. Thus, T_{NI} of PAPB*n* with an odd number of n was lower than those of an even number of n. These odd–even effects have been commonly observed in various LC systems.[21,22] In Figures 5 and 6, of note are the particularly low values of T_{NI}, ΔH_{NI}, and ΔS_{NI} of PAPB3. A similar specific feature has been pointed out in a series of poly(methacrylates) with side-chain cyano-

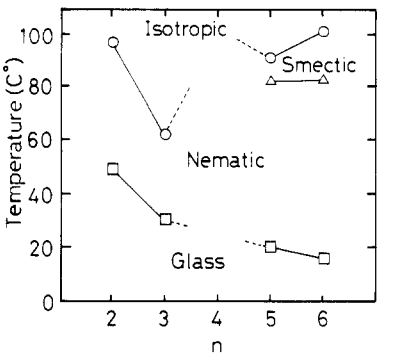

Figure 5. Phase transition temperatures of PAPB*n* (M_n = ~4000) as a function of the number of methylene units in the spacer chains.

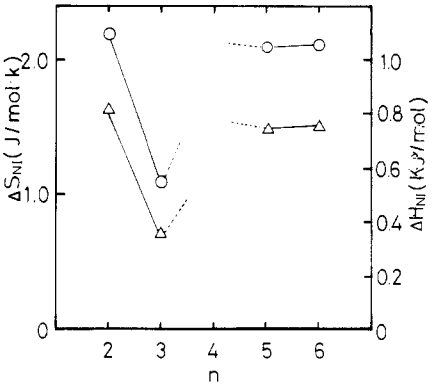

Figure 6. Change in enthalpy and entropy at N–I phase transition (ΔH_{NI} and ΔS_{NI}) for PAPB*n* (M_n = ~4000) as a function of the number of methylene units in the spacer chains: (○), ΔS_{NI}; (△), ΔH_{NI}

biphenyl mesogens.[23] It is now widely accepted that the odd–even effects observed for LC's with flexible alkyl chains can be explained in terms of spatial orientation of the mesogens linked by the alkyl spacers.[24] Thus, the mesogens linked by the even-numbered methylene units adopt a rather parallel orientation, while the mesogens linked by the odd-numbered methylene units are bent to the same direction if we assume a trans–trans conformation of the methylene units in the alkyl chains. This bent form of the mesogens is expected to weaken the mutual interaction in the mesogenic phase, leading to a less ordered structure of the liquid crystals. In the case of the side-chain PLC's, an additional effect should be taken into account. Because of the short alkyl spacer, the mesogens in PAPB3 are not sufficiently isolated from the main chain of the polymers; thus they are strongly influenced by the conformation of the main chain. Usually, in polyacrylates the main chains possess a tendency to take random orientation so that the mesogens in PAPB3 are affected in such a way that they take random orientation as well.

Phase Transition Behaviors of PAPB*n* Doped with BMAB. In the subsequent paper,[25] we studied the photochemically induced phase transition behaviors of PAPB*n* doped with a photochromic compound, 4-*n*-butyl-4′-methoxyazobenzene (BMAB), in full detail. We found that isothermal N–I phase transition could be successfully induced by the photoisomerization of BMAB doped in the homopolymers. In order to explore the photochemically induced phase transition behaviors, we studied the thermotropic properties of PAPB*n* doped with BMAB.

In Figure 7, T_g and T_{NI} of PAPB3 (M_n = 3000) doped with BMAB (k32n42i) are shown as a function of the

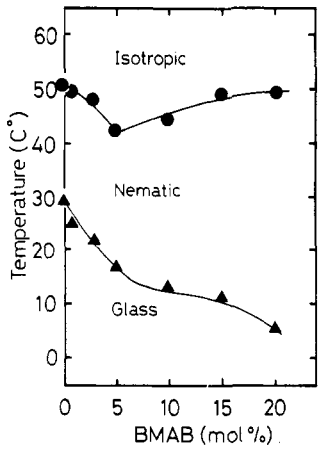

Figure 7. Phase transition temperatures of PAPB3 (M_n = 3000) as a function of the concentration of the doped BMAB.

concentration of the doped BMAB. T_g of the mixture decreased monotonically with the amount of the doped BMAB. This may be interpreted in terms of the assumption that BMAB acts as a plasticizer. T_{NI} of the mixture changed in a peculiar way. At the concentration of 5 mol %, the mixture showed the lowest value of T_{NI}, and above this concentration T_{NI} increased gradually.

Table I shows the phase transition behaviors of the other homopolymers doped with 5 mol % of BMAB. MW of the samples was ~4000. The data for PAPB3 with M_n = 4000 were added for comparison. In these systems, detailed concentration dependence was not investigated since the photochemically induced phase transition did not take place. In all mixtures, T_g, T_{NI}, and T_{SN} were lower than those of the pure homopolymers.

Phase Transition Behaviors of Copolymers. Phase transition behaviors were investigated of copolymer *n*–*m* in which *n* was fixed mainly to 3 and *m* was varied as 2, 3, 5, 6, or 11. As shown in Table II, all the samples of copolymer 3–*m* exhibited the liquid crystalline phase (N). In order to compare the photochemically induced phase transition behavior between copolymer *n*–*m* and PAPB*n* doped with BMAB, the composition of the copolymers was designed so as to be similar to those of the doped systems. Namely, in the doped systems, the concentration of the doped BMAB was usually 5 mol %; thus the content of the azo monomer (AAZO*m*) in the copolymers was intended to be as close as possible to 5 mol %. Table II also indicates the MW dependence of the phase transition temperature. As in the case of the homopolymers, T_g and T_{NI} increased with increasing MW, while ΔH_{NI} and ΔS_{NI} remained nearly unchanged in copolymer 3–*m* with *m* = 2, 3, or 11 and increased in copolymer 3–*m* with *m* = 5 or 6.

In Figure 8 are shown the phase transition temperatures (T_g and T_{NI}) of copolymer 3–*m* with M_n = ~4000 as a function of the number of the methylene units in the spacer chain attached to the azobenzene moiety (*m*). In this figure, the phase transition temperatures of PAPB3 doped with 5 mol % of BMAB are also included for comparison. It can be seen that T_{NI} is insensitive to the alkyl chain length (*m*) in copolymer 3–*m*. T_g of copolymer 3–*m* is also insensitive to the alkyl spacer length, although it tends to decrease with increasing *m*.

Contrary to the behavior of T_g and T_{NI}, both ΔH_{NI} and ΔS_{NI} are strongly dependent on the alkyl spacer length *m* as shown in Figure 9. Copolymer 3–3 possessed the lowest values of both ΔH_{NI} and ΔS_{NI} among the copolymers and the homopolymer PAPB3 doped with BMAB. Table III shows the effect of the composition of copolymer 3–3 on the phase transition behaviors. One can see that with increasing the azo monomer content, T_g, T_{NI}, ΔH_{NI}, and ΔS_{NI} decreased.

Order Parameters Determined by IR Dichroism. For a uniaxially symmetrical system such as a nematic phase, the dichroic ratio, *R*, can be given by eq 1,[26] where

$$R = \frac{\epsilon_\parallel}{\epsilon_\perp} = \frac{(4\cos^2\alpha)\langle\cos^2\theta\rangle + (2\sin^2\alpha)\langle\sin^2\theta\rangle}{(2\cos^2\alpha)\langle\sin^2\theta\rangle + (\sin^2\alpha)\langle 1 + \cos^2\theta\rangle} \quad (1)$$

$\epsilon_\parallel$ and $\epsilon_\perp$ are the absorption coefficients measured with the IR beam polarized parallel and perpendicular to the optical axis of the molecule, respectively. Furthermore, θ is the angle between the direction of the long axis of the molecule and the optical axis of the uniformly oriented liquid crystal and α is the angle between the long axis of the molecule and the direction of the vibrational transition moment. In case where the vibrational transition moment is oriented parallel to the long axis of the molecule, the order parameter, *S*, can be written in the form of eq 2.[26]

$$S = \frac{R - 1}{R + 2} \quad (2)$$

Figure 10 shows the FT-IR polarized absorption spectra of PAPB5 measured at 25 °C. The sample film was oriented in the magnetic field. A peak at 1720 cm^{-1} is due to C=O stretching vibration, and two peaks at 1600 and 1500 cm^{-1} are assigned to the C=C stretching mode of aromatics. In the two peaks assigned to the aromatic C=C stretching vibration, $\epsilon_\parallel$ is much larger than $\epsilon_\perp$, which is apparently a consequence of the parallel orientation of the corresponding vibrational transition moment for these absorption bands to the molecular long axis.[27] On the other hand, in the peak at 1720 cm^{-1} $\epsilon_\parallel$ is smaller than $\epsilon_\perp$, which is interpreted in terms of rather perpendicular orientation of the transition moment of the C=O stretching vibration to the molecular long axis.[28] We used the peak at 1600 cm^{-1} for the determination of the order parameters of the PLC's.

In Figure 11 are shown the order parameters, *S*, of PAPB5 (M_n = 3900) as a function of the reduced temperature ($T_{red.} = T/T_{NI}$). Two series of plots are indicated: one is for the sample oriented by the rubbing treatment (●) and the other is oriented in the magnetic field (○). It is evident that the values of *S* of the sample oriented by the rubbing treatment are smaller than those oriented in the magnetic field. This tendency was observed in other polymers. Futhermore, reproducibility in *S* was much worse in the samples prepared by the rubbing treatment. Repeated measurements gave a difference in *S* by 0.1~0.2 even in the same samples. This indicates clearly that by the rubbing treatment preparation of the uniformly oriented samples of PLC is rather difficult; thus determination of *S* was performed for the samples oriented in the magnetic field in the following.

Figure 12 shows the order parameters of PAPB*n* with M_n = ~4000 as a function of the reduced temperature. An abrupt change in *S* corresponds to the phase transition. It is seen that PAPB3 possesses lower values of *S* than the other polymers approximately in the whole temperature range. Coupled with the extraordinarily low values of the thermodynamic parameters (T_{NI}, ΔH_{NI}, and ΔS_{NI}) of PAPB3, this result clearly indicates that PAPB3 has a much less ordered structure in the N state than the other homopolymers. A parallel tendency between ΔS_{NI} and *S* can be rationalized if we assume that PLC's have the same values of entropy in the isotropic state.

Table I
Thermodynamic Properties of PAPBn Doped with BMAB

n	M_n	M_w/M_n	[BMAB], mol %	phase transitn temp, °C	ΔH_{SN}, kJ/mol	ΔS_{SN}, J/(mol K)	ΔH_{NI}, kJ/mol	ΔS_{NI}, J/(mol K)
2	3600	1.29	0	g47n93i			0.65	1.77
			5	g38n88i			0.64	1.78
3	4000	1.18	0	g26n63i			0.35	1.05
			5	g17n61i			0.25	0.75
5	3900	1.17	0	g20s83n93i	1.99	5.60	0.77	2.10
			5	g8s66n82i	1.51	4.45	1.00	2.82
6	3900	1.22	0	g14s82n101i	0.96	2.69	0.76	2.02
			5	g7s70n94i	0.80	2.31	0.96	2.60

Table II
Thermodynamic Properties of Copolymer *n*–*m*

n	m	M_n	M_w/M_n	[AZO], mol %	phase transitn temp, °C	ΔH_{SN}, kJ/mol	ΔS_{SN}, J/(mol K)	ΔH_{NI}, kJ/mol	ΔS_{NI}, J/(mol K)
3	2	3300	1.17	4.2	g23n54i			0.21	0.65
	2	4100	1.25	4.2	g33n63i			0.21	0.63
3	3	3500	1.23	3.8	g30n63i			0.18	0.53
	3	6000	1.39	3.8	g36n69i			0.18	0.52
3	5	4800	1.21	3.8	g27n62i			0.25	0.75
	5	5400	1.29	3.8	g29n70i			0.29	0.83
3	6	3800	1.23	5.0	g28n59i			0.29	0.86
	6	5800	1.39	5.0	g30n63i			0.39	1.17
3	11	3500	1.13	6.2	g23n63i			0.36	1.07
	11	4500	1.19	6.2	g25n66i			0.36	1.06
6	3	6000	1.36	4.2	g24s82n112i	0.75	2.12	0.99	2.57
6	6	6900	1.35	5.9	g21s89n116i	0.91	2.52	0.91	2.35

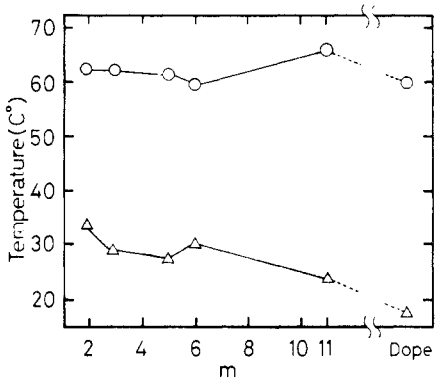

Figure 8. Phase transition temperature of copolymer 3-*m* (M_n = ~4000) as a function of the number of methylene units in the spacer chain attached to the azobenzene moiety: (○), T_{NI}; (△), T_g.

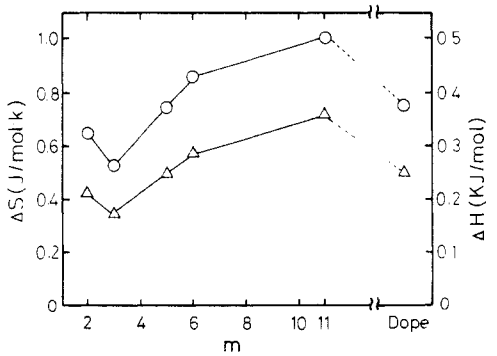

Figure 9. Change in enthalpy and entropy at N–I transition of copolymer 3-*m* (M_n = ~4000) as a function of the number of methylene units in the spacer chain length attached to the azobenzene moiety: (○), ΔS_{NI}; (△), ΔH_{NI}.

Namely, a large value of ΔS_{NI} means a small value of entropy in the N state and thus higher orientational ordering in the N state. Such a parallel relationship has been already reported for main-chain PLC's[29,30] and low MW liquid crystals.[31]

In Figure 13 are shown the values of S for copolymer 3-*m* with various *m*'s as a function of the reduced temperature. It is evident that the S values of copolymer 3-3 are much lower than those of copolymer 3-6 and copolymer 3-11 over the temperature range examined. Furthermore, the plots for the doped PLC film (PAPB3/BMAB; ●) explicitly reveal that at lower temperatures the S values for this film are higher than any of the copolymers studied; however, at temperatures close to $T_{red.}$ = 1, the S values dropped abruptly.

4,4'-Disubstituted azobenzene derivatives can form LC phase; however, their ability to form LC phase is rather

Table III
Thermodynamic Properties of Copolymer 3-3 with Various Azo Contents

[azo], mol %	M_n	M_w/M_n	phase transitn temp, °C	ΔH_{NI}, kJ/mol	ΔS_{NI}, J/(mol K)
3.8	3500	1.23	g30n63i	0.18	0.53
3.8	6000	1.39	g36n69i	0.18	0.52
9.4	4300	1.15	g26n57i	0.14	0.43
9.4	5000	1.25	g32n67i	0.21	0.63
12.0	5500	1.29	g29n57i	0.14	0.43
12.0	7800	1.28	g32n61i	0.11	0.32

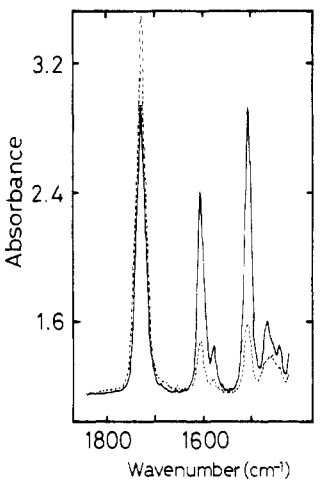

Figure 10. FT-IR polarized absorption spectra of PAPB5 at 25 °C (M_n = 3900): (–), polarized parallel to the optical axis; (···), polarized perpendicular to the optical axis.

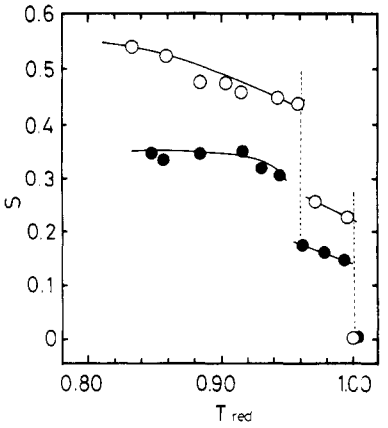

Figure 11. Order parameter of PAPB5 determined by FT-IR dichroism as a function of $T_{red.}$: (●), oriented by rubbing treatment; (○), oriented in the magnetic field.

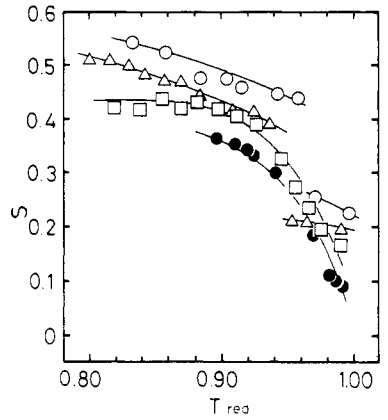

Figure 12. Order parameters of PAPBn determined by FT-IR dichroism as a function of $T_{red.}$: (□), PAPB2; (●), PAPB3; (○), PAPB5; (△), PAPB6.

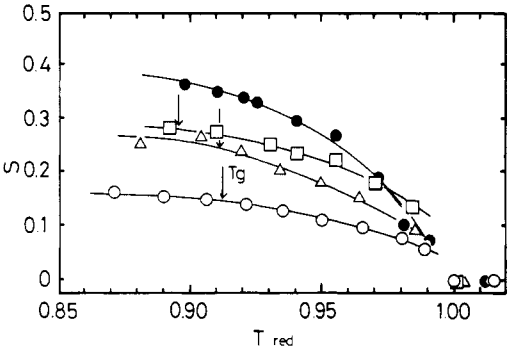

Figure 13. Order parameters of copolymer 3–*m* and PAPB3 doped with BMAB (5 mol %) as a function of $T_{red.}$ (M_n = 4000): (○), copolymer 3–3; (△), copolymer 3–6; (□), copolymer 3–11; (●), PAPB3 doped with BMAB.

low because of weak interaction between the azobenzene moieties.[32] Thus, incorporation of azobenzene derivatives into mesogenic phases may result in a less ordered structure of the host mesogens. Validity of this assumption is confirmed. As can be seen in Table III, T_{NI} as well as ΔH_{NI} and ΔS_{NI} decrease with increasing azo monomer content. Furthermore, among copolymer 3–*m* one with m = 3 exhibited the lowest values of ΔS_{NI} and S, which is another piece of evidence that the azobenzene moiety weakens interaction between phenyl benzoate mesogens when incorporated with the same spacer length as the phenyl benzoate mesogens.

Conclusion

Orientational ordering in the side-chain PLC's with mesogenic phenyl benzoate moieties has been explored for the homopolymers with different spacer length, PAPB*n*, and the copolymers containing photoresponsive azobenzene moieties, poly(APB*n*-*co*-AAZO*m*) (copolymer *n*–*m*), by means of the calorimetric measurements and the order parameter determinations by FT-IR dichroism. A parallel relationship between ΔS_{NI} and S (order parameter) of the matrix PLC's has been confirmed: a system with a small value of ΔS_{NI} shows a small value of S, indicating a disordered system. Among the homopolymers, PAPB3 exhibited the lowest value of ΔS_{NI} and S. When a photoresponsive azobenzene derivative (BMAB) was incorporated into PAPB3, the resulting mixture showed a further decrease in ΔS_{NI} and S compared with those of the pure homopolymer. Among the copolymers examined, copolymer 3–3 possessed the lowest values of ΔS_{NI} and S, indicating the least ordered structure of the copolymer in the LC state. Furthermore, copolymer 3–3 exhibited smaller values of ΔS_{NI} and S than PAPB3/BMAb; thus this copolymer has the most disordered structure among the PLC samples examined in this study.

Registry No. $PAPB_2$ (homopolymer), 79462-29-6; $PAPB_3$ (homopolymer), 118086-64-9; $PAPB_5$ (homopolymer), 118086-66-1; $PAPB_6$ (homopolymer), 82200-54-2; $(APB_3)(AAZO_2)$ (copolymer), 123642-70-6; $(APB_3)(AAZO_3)$ (copolymer), 123642-72-8; $(APB_3)(AAZO_5)$ (copolymer), 123642-74-0; $(APB_3)(AAZO_6)$ (copolymer), 123642-76-2; $(APB_3)(AAZO_{11})$ (copolymer), 123642-78-4.

References and Notes

(1) Yoshizawa, T. *Adv. Biophys.* **1984**, *17*, 5.
(2) Tazuke, S.; Kurihara, S.; Yamaguchi, H.; Ikeda, T. *J. Phys. Chem.* **1987**, *91*, 249.
(3) Yamaguchi, H.; Ikeda, T.; Tazuke, S. *Chem. Lett.* **1988**, 539.
(4) Tazuke, S.; Kurihara, S.; Ikeda, T. *Chem. Lett.* **1987**, 911.
(5) Ikeda, T.; Horiuchi, S.; Karanjit, D. B.; Kurihara, S.; Tazuke, S. *Chem. Lett.* **1988**, 1679.
(6) Kurihara, S.; Ikeda, T.; Tazuke, S. *Jpn. J. Appl. Phys., Part 2* **1988**, *27*, L1791.
(7) Stolka, M.; Yanus, J. F.; Pai, D. M. *J. Phys. Chem.* **1984**, *88*, 4707.
(8) Borsenberger, P. M.; Mey, W.; Chowdry, A. *J. Appl. Phys.* **1978**, *49*, 273.
(9) Pfister, G. *Phys. Rev. B: Solid State* **1977**, *16*, 3676.
(10) Tazuke, S.; Hayashi, N. *J. Polym. Sci., Polym. Chem. Ed.* **1978**, *16*, 2729.
(11) Shibaev, V. P.; Kostromin, S. G.; Plate, N. A.; Ivanov, S. A.; Vetrov, V. Y.; Yakovlev, I. A. *Polym. Commun.* **1983**, *24*, 364.
(12) Coles, H. J.; Simon, R. *Polymer* **1985**, *26*, 1801.
(13) Sasaki, A. *Mol. Cryst. Liq. Cryst.* **1986**, *139*, 103.
(14) Pinsl, J.; Brauchle, C.; Kreuzer, F. H. *J. Mol. Electron.* **1987**, *3*, 9.
(15) Eich, M.; Wendorff, J. H.; Reck, B.; Ringsdorf, H. *Makromol. Chem., Rapid Commun.* **1987**, *8*, 59.
(16) Eich, M.; Wendorff, J. H. *Makromol. Chem., Rapid Commun.* **1987**, *8*, 467.
(17) Portugall, M.; Ringsdorf, H.; Zental, R. *Makromol. Chem.* **1982**, *183*, 2311.
(18) Ringsdorf, H.; Schmidt, H.-W. *Makromol. Chem.* **1984**, *185*, 1327.
(19) Stevens, H.; Rehage, G.; Finkelmann, H. *Macromolecules* **1984**, *17*, 851.
(20) Blumstein, R. B.; Stickles, E. M.; Blumstein, A. *Mol. Cryst. Liq. Cryst.* **1982**, *82*, 205.
(21) Roveillo, A.; Sirigu, A. *Makromol. Chem.* **1982**, *183*, 895.
(22) Vanmeter, J. P.; Klanderman, B. H. *Mol. Cryst. Liq. Cryst.* **1973**, *22*, 271.
(23) Noel, C. *IUPAC Symp. Macromol., Kyoto, Prepr.* **1988**, 486.
(24) Abe, A. *Macromolecules* **1984**, *17*, 2280.
(25) Ikeda, T.; Horiuchi, S.; Karanjit, D. B.; Kurihara, S.; Tazuke, S. *Macromolecules*, following paper in this issue.

(26) Neff, V. D. In *Liquid Crystals and Plastic Crystals*; Gray, G. W., Winsor, P. A., Eds.; Ellis Horwood: Chichester, 1974; Vol. 2, pp 231-253.
(27) Noel, C.; Laupretre, F.; Friedrich, C.; Fayolle, B.; Bosio, L. *Polymer* **1984**, *25*, 808.
(28) Landreth, B. M.; Stupp, S. I. *Macromolecules* **1987**, 2083.
(29) Watanabe, J.; Krigbaum, W. R. *Macromolecules* **1984**, *17*, 2288.
(30) Iimura, K.; Koide, N.; Ujiie, S. *11th Liq. Cryst., Int. Conference, 11th* **1986**, θ-112-M5.
(31) Toriumi, H.; Furuya, H.; Abe, A. *Polym. J. (Tokyo)* **1985**, *17*, 895.
(32) Konstantinov, I. *J. Phys. (Les Ulis, Fr.)* **1979**, *40*, C3-475.

Photochemically Induced Isothermal Phase Transition in Polymer Liquid Crystals with Mesogenic Phenyl Benzoate Side Chains. 2. Photochemically Induced Isothermal Phase Transition Behaviors

Tomiki Ikeda,* Shin Horiuchi, Durga B. Karanjit, Seiji Kurihara, and Shigeo Tazuke†

Photochemical Process Division, Research Laboratory of Resources Utilization, Tokyo Institute of Technology, 4259 Nagatsuta, Midori-ku, Yokohama 227, Japan.
Received October 3, 1988; Revised Manuscript Received April 20, 1989

ABSTRACT: Photochemically induced isothermal phase transition in polymer liquid crystals (PLC) with mesogenic phenyl benzoate side chains has been demonstrated. PLC's examined are poly(4′-methoxyphenyl 4-((acryloyloxy)alkoxy)benzoate) (PAPB*n*), in which the alkyl spacer length $(CH_2)_n$ was varied as n = 2, 3, 5, or 6 and their copolymers with 4′-methoxy-4-((acryloyloxy)alkoxy)azobenzene (AAZO*m*) where m = 2, 3, 5, 6, or 11 (poly(APB*n*-*co*-AAZO*m*) or copolymer *n*-*m*). Two types of systems have been explored: one is composed of PAPB*n* doped with a small amount of a low molecular weight (MW) mesogen with a photoresponsive moiety, 4-butyl-4′-methoxyazobenzene (BMAB), and the other is copolymer *n*-*m*. Photoirradiation of the PAPB3/BMAB (5 mol %) film at 366-nm light caused the trans → cis isomerization of BMAB, which induced simultaneously the nematic (N) → isotropic (I) phase transition of the PLC film. This process was reversible, and photoirradiation at 525 nm which induced the cis → trans isomerization of BMAB restored the system to the initial phase (N). The phase transition behavior was found to be strongly dependent on the spacer length (*n*) and MW of the PLC. Similar isothermal phase transition behaviors were observed in copolymer 3-*m*; however, in other copolymers like copolymer 6-*m* the isothermal phase transition could not be induced photochemically. Among the PLC samples examined, copolymer 3-3 showed the highest rate of isothermal phase transition. On the basis of the calorimetric studies and order parameter determinations reported in the preceding paper, the efficiency of the photochemically induced isothermal phase transition was found to be closely related to orientational ordering of the initial state of the PLC. Thus, the N → I isothermal phase transition took place more effectively in a system with a less ordered N state. Resolution of the stored image was estimated as 2∼4 μm on the basis of experiments where copolymer 3-3 was covered with a photomask and irradiated with the third harmonic of a YAG laser.

Introduction

Liquid crystals (LC) have been most extensively used as display materials. Successful application of the LC display cells covers the numerical data displays for wrist watches and calculators, sentence displays for word processors, and full-color TV displays. The function of these display cells are essentially based on the electrooptic effect of the LC, requiring a matrix arrangement of the transparent electrodes.[1,2] Thus, a high resolution over a large area is a tough problem for these LC cells to overcome.[2]

A laser beam addressed display has been recently developed.[1,2] This is principally based on the thermooptic effects of the LC's, and frequently electrothermooptic effects are also employed. Since the laser beam can be focused to <10-μm diameter, high resolution can be expected for the laser beam addressed displays.[2] The write-in process includes irradiation of the LC cells with a laser beam, a rapid increase in temperature along the laser beam trace results in a phase transition from the liquid crystalline state (nematic (N) or smectic (S)) to the isotropic (I) state, and removal of the laser beam leads to rapid cooling of the isotropic trace, producing light scattering centers such as honeycomb and focal conic textures.[2] These light scattering centers remain in the LC cells; thus they can display static figures. However, stability of the stored information is not satisfactory, and the high contrast will be lost after some period.[1,2]

The use of polymer liquid crystals (PLC) as optical storage materials has become a current topic in view of the glass transition (T_g) phenomenon and processability of polymers. Cell-free polymer films with the ability of long-term information storage are evidently favored from an industrial viewpoint. The laser beam addressed recording has been achieved in side-chain PLC's[3-5] and in main-chain PLC.[6] They are mainly based on the thermooptic effects, but photochemical reactions play an important roll in the write-once storage materials.[5]

Photon-mode optical image storage in PLC's has been demonstrated by Eich and Wendorff.[7,8] Their system is composed of PLC's with side-chain photochromic azoben-

† Deceased July 11, 1989.

0024-9297/90/2223-0042$02.50/0